I
Linear and Non-linear Properties of Photonic Crystals

Nanophotonic Materials: Photonic Crystals, Plasmonics, and Metamaterials. Edited by R.B. Wehrspohn, H.-S. Kitzerow, and K. Busch

ISBN: 978-3-527-40858-0

1
Solitary Wave Formation in One-dimensional Photonic Crystals

Sabine Essig, Jens Niegemann, Lasha Tkeshelashvili, and Kurt Busch

1.1
Introduction

Periodically modulated dielectric structures exhibit the peculiar property that their multibranch dispersion relations may be separated by Photonic Band Gaps (PBGs) [1,2]. In the linear regime, optical waves with frequencies within these PBGs cannot propagate inside the sample and decay exponentially with distance. This gives rise to a number of novel physical phenomena that have significant potential for applications in telecommunication and all-optical information processing.

In the case of nonlinear periodic structures, the physics exhibits a much richer behavior [3]. For instance, due to the optical Kerr effect, i.e., an intensity-dependent refractive index, sufficiently intense electromagnetic pulses can locally tune the PBG. As a consequence, the system may become transparent to optical waves with frequencies in the (linear) band gaps. Moreover, in the presence of optical nonlinearities, modulational instabilities of these waves may occur. This leads to novel types of solitary excitations in PBG materials, the so-called gap solitons. Gap solitons have first been discovered by Chen and Mills [4], and are characterized by a central pulse frequency within a photonic band gap. Most notably, gap solitons can possess very low and even vanishing propagation velocities and, thus, lend themselves to various applications for instance in optical buffers and delay lines as well as in information processing. It should be noted that PBG materials allow solitary waves with carrier frequencies outside the band gaps, too. Such pulses are generally referred to as Bragg solitons [3]. To date, low group velocity Bragg solitons have been observed in fiber Bragg gratings [5,6]. These systems represent a very important class of (quasi) one-dimensional PBG materials which has already found many applications in various areas of photonics. In the following, we, therefore, concentrate on an analysis of fiber Bragg gratings. However, we would like to emphasize that owing to the universal nature of nonlinear wave propagation phenomena our results are of relevance for a number of physical

Nanophotonic Materials: Photonic Crystals, Plasmonics, and Metamaterials. Edited by R.B. Wehrspohn, H.-S. Kitzerow, and K. Busch

ISBN: 978-3-527-40858-0

systems ranging from two- or three-dimensional photonic crystals all the way to Bose–Einstein condensates in optical lattices.

The appropriate theoretical model to describe nonlinear wave phenomena in one-dimensional PBG materials is the so-called coupled mode theory [3]. In this model, forward and backward propagating waves are described through appropriate carrier waves that are modulated with corresponding (slowly varying) envelopes $E_{\pm}$. The resulting equations of motions for these envelopes are

$$i\frac{\partial E_+}{\partial z} + i\frac{\partial E_+}{\partial t} + E_- + |E_+|^2 E_+ + 2|E_-|^2 E_+ = 0, \tag{1.1a}$$

$$-i\frac{\partial E_-}{\partial z} + i\frac{\partial E_-}{\partial t} + E_+ + |E_-|^2 E_- + 2|E_+|^2 E_- = 0. \tag{1.1b}$$

Equations (1.1a) and (1.2b) are generally known as Nonlinear Coupled Mode Equations (NLCME). The NLCME are given in dimensionless variables, and the nonlinearity is assumed to be positive. For a detailed discussion of the NLCME, including their derivation directly from Maxwell's equations, we refer to Ref. [3]. Below, we will only give a brief synopsis of those results on the NLCME that pertain to our work on solitary wave formation described in Sections 1.2 and 1.3.

The coupled mode theory only accounts for one band gap located between two bands, an upper and a lower band, respectively. For systems such as fiber Bragg gratings, the NLCME provide a very accurate framework for studying nonlinear wave dynamics [5]. Although NLCME are nonintegrable, there are known exact solitary wave solutions to these equations which read as [3]

$$E_{\pm}(z,t) = \alpha\tilde{E}_{\pm}(z,t)e^{i\eta(\theta)}. \tag{1.2}$$

Here, $\tilde{E}_{\pm}$ represent the one-soliton solutions of the massive Thirring model which corresponds to the NLCMEs without self-phase modulations terms [3]. Explicitly, these one-soliton solutions read as

$$\tilde{E}_+ = \sqrt{\frac{1}{2}}\frac{1}{\Delta}\sin\delta\, e^{i\sigma}\sec h(\theta - i\delta/2), \tag{1.3a}$$

$$\tilde{E}_- = -\sqrt{\frac{1}{2}}\Delta\, \sin\delta\, e^{i\sigma}\sec h(\theta + i\delta/2), \tag{1.3b}$$

where we have introduced the abbreviations

$$\theta = \gamma(z - vt)\sin\delta, \qquad \sigma = \gamma(vz - t)\cos\delta, \tag{1.4}$$

as well as

$$\Delta = \left(\frac{1-v}{1+v}\right)^{\frac{1}{4}}, \qquad \gamma = \frac{1}{\sqrt{1-v^2}}. \tag{1.5}$$

Finally, α and $\eta(\theta)$ are given by

$$\frac{1}{\alpha^2} = 1 + \frac{1+\nu^2}{2(1-\nu^2)}, \qquad e^{i\eta} = \left(-\frac{e^{2\theta} + e^{\mp i\delta}}{e^{2\theta} + e^{\mp i\delta}} \right)^{\frac{2\nu}{3-\nu^2}}. \tag{1.6}$$

These solutions (1.2) of the NLCME depend on two independent parameters, the detuning δ and the scaled group velocity ν. The scaled group velocity can take on any value below the speed of light (i.e., $-1 \leq \nu \leq +1$) and may even vanish. The latter case corresponds to stationary solutions which have been found by Chen and Mills [4] through numerical experiments. The detuning δ of the soliton describes the value of the waves' central (carrier) frequency relative to the band edge and varies over a range $0 \leq \delta \leq \pi$. If δ is close to zero, the spectrum of the solitary wave is concentrated around the upper band edge (in the case of positive nonlinearity). The Bragg frequency associated with the center of the band gap corresponds to a detuning $\delta = \pi/2$. At this point, we would like to note that in terms of our dimensionless units the photonic band gap is located in the interval $[-1, 1]$. Equation (1.3) describes both gap and Bragg solitons. A stability analysis of these solitary wave solutions has shown that pulses with $\delta < \pi/2$ remain stable against small perturbations. However, for detuning $\delta > \pi/2$, the solitary waves become unstable and decay to radiation modes after a certain transient time [7].

In any realistic experimental situation, the exact soliton-shaped pulses cannot be launched directly. Instead, a formation of a solitary wave has to take place starting with an initial pulse with "distorted" shape that radiates away the excess energy into low amplitude linear modes. The influence of the PBG on this reshaping process is expected to be drastically increased for small values of the detuning. As alluded to above, for $\delta \to 0$ the spectrum of the pulse is mostly concentrated at the band edge where the group velocity of the eigenmodes is very small or even zero. Therefore, the linear waves (not to be confused with the linear eigenmodes) radiated from the initial nonlinear pulse will be strongly back-scattered by the PBG material. In turn, this will cause pronounced memory effects (also called non-Markovian effects; see the discussion in Section 1.3) in the soliton formation process quite similar to the atom-photon interaction processes in PBG materials [8,9]. This is the starting point of our analysis in the present paper. Owing to the non-integrability of the NLCME, we study this problem by means of a variational approach. We describe the details of this variational approach to the NLCME and how to include a coupling of the nonlinear radiation modes to linear losses in Sections 1.2 and 1.3, respectively. In Section 1.4, we report about results and comparison with numerically exact calculations. Finally, we summarize our findings in Section 1.5, where we also provide a perspective on improved treatments of losses within the NLCME.

1.2 Variational Approach to the NLCME

The variational approach to the NLCME is based on the Lagrangian density of the system in non-dimensional form

$$\begin{aligned}\mathcal{L} = \frac{i}{2}\Bigg[& E_+^*\left(\frac{\partial}{\partial t}+\frac{\partial}{\partial z}\right)E_+ - E_+\left(\frac{\partial}{\partial t}+\frac{\partial}{\partial z}\right)E_+^* \\ & + E_-^*\left(\frac{\partial}{\partial t}-\frac{\partial}{\partial z}\right)E_- - E_-\left(\frac{\partial}{\partial t}-\frac{\partial}{\partial z}\right)E_-^*\Bigg] \\ & + \frac{1}{2}|E_+|^4 + \frac{1}{2}|E_-|^4 + 2|E_+|^2|E_-|^2 + E_+^*E_- + E_+E_-^*.\end{aligned} \tag{1.7}$$

The action corresponding to this Lagrangian density is invariant under temporal and spatial translations as well as under phase transformations. According to the Noether Theorem, every symmetry transformation generates a corresponding conserved quantity [10]. In our subsequent analysis, the mass and energy conservation laws are of major importance. The mass conservation law reads

$$\int_{-\infty}^{\infty}\left(|E_+|^2+|E_-|^2\right)\mathrm{d}z = \text{const}, \tag{1.8}$$

whereas the energy conservation law states

$$\begin{aligned}\int_{-\infty}^{\infty}\Bigg(\frac{i}{2}\Bigg[& E_+^*\frac{\partial E_+}{\partial z} - E_+\frac{\partial E_+^*}{\partial z} - E_-^*\frac{\partial E_-}{\partial z} + E_-\frac{\partial E_-^*}{\partial z}\Bigg] \\ & + \frac{1}{2}|E_+|^4 + \frac{1}{2}|E_-|^4 + 2|E_+|^2|E_-|^2 + E_+^*E_- + E_+E_-^*\Bigg)\mathrm{d}z = \text{const}.\end{aligned} \tag{1.9}$$

According to the general scheme for variational approach [11], we have to choose the trial functions for the forward and backward propagating modes of the NLCME that are tailored towards the problem under consideration. In the present case, our Ansatz must allow the pulse to relax to the exact gap soliton shape. For simplicity, we restrict ourselves to the evolution of stationary gap solitons, i.e., we choose the scaled group velocity v to be zero. Other situation can be treated analogously, albeit with considerably more complex notations. In addition, the trial functions must also contain a radiation part. Based on these considerations, we formulate the following Ansatz

$$E_+(z,\,t) = +\left[\eta_+(t)\,\mathrm{sec}\,h\left(\sin\delta_+(t)z - \frac{i}{2}\delta_+(t)\right) + ig_+(t)\right]\mathrm{e}^{-ia_+(t)}, \tag{1.10a}$$

$$E_-(z,\,t) = -\left[\eta_-(t)\,\mathrm{sec}\,h\left(\sin\delta_-(t)z + \frac{i}{2}\delta_-(t)\right) + ig_-(t)\right]\mathrm{e}^{-ia_-(t)} \tag{1.10b}$$

together with the initial conditions

$$E_+(z,\,t=0) = +\eta_0\,\mathrm{sec}\,h\left(\sin\delta_0 - \frac{i}{2}\,\delta_0\right), \tag{1.11a}$$

$$E_-(z,\,t=0) = -\eta_0\,\mathrm{sec}\,h\left(\sin\delta_0 + \frac{i}{2}\,\delta_0\right), \tag{1.11b}$$

where the initial amplitudes and detunings of the forward and backward propagating modes are chosen to be the same. The (time-dependent) variational parameters

are the amplitudes $\eta_\pm$, the detunings $\delta_\pm$, the so-called shelf functions $g_\pm$, and the phases $a_\pm$. The first part of the trial function describes the initial pulse and the second part, consisting of the functions $g_\pm$, describes the nonlinear radiation modes. In our case, the shelf functions $g_\pm$ are of particular importance, since they allow the localized pulse to couple to linear radiation modes. Far away from the nonlinear pulse, the system dynamics is essentially linear so that the nonlinear extended modes can only contribute in a spatial region of finite extent around the pulse. As a consequence, the shelf should have a finite length l. Furthermore, in view of the symmetry between E_+ and E_- and inspired by numerically exact solutions of the NLCME, we assume

$$\eta_+ = \eta_- = \eta, \tag{1.12a}$$

$$\delta_+ = \delta_- = \delta, \tag{1.12b}$$

$$g_+ = g_- = g, \tag{1.12c}$$

$$a_+ = a_- = a, \tag{1.12d}$$

so that there are only four independent variational parameters in our problem.

Now, we insert the trial function given, Eqs. (1.10a) and (1.10b), into the Lagrangian density, Eq. 1.7, and carry out the integration over all space. As a result, we derive the effective Lagrangian of the system

$$\begin{aligned} L_{\text{eff}} = {} & 4\eta^2 \frac{\delta}{\sin^2\delta}\frac{da}{dt} - 2\pi\eta\frac{1}{\sin\delta}\frac{dg}{dt} - 4\eta^2\frac{1}{\sin\delta}(1-\delta\cot\delta) - 2\pi g\eta\frac{\cot\delta}{\sin\delta}\frac{d\delta}{dt} \\ & + 2\pi g\frac{1}{\sin\delta}\frac{d\eta}{dt} + 2g^2 l\frac{da}{dt} + 12\eta^4\frac{1}{\sin^3\delta}(1-\delta\cot\delta) + 4\eta^2 g^2\frac{1}{\sin\delta} \\ & + 3g^4 l + 8\eta^2 g^2\frac{\delta}{\sin^2\delta} - 4\eta^2\frac{1}{\sin\delta} - 2g^2 l. \end{aligned} \tag{1.13}$$

Using this expression, we obtain the following equations of motion for the four independent variational parameters η, δ, g, and a

$$\begin{aligned} \frac{d\eta}{dt} = {} & \frac{g}{\pi}\Bigg(-l\delta - 2\eta^2 - l\delta\cos^2\delta + 9\eta^2 l\delta\cot^2\delta - 4\eta^2\frac{\delta}{\sin\delta} + 3l\eta^2\frac{\delta}{\sin^2\delta} \\ & + l\sin\delta - g^2 l\sin\delta - 2l\delta\cos\delta + g^2 l\cos\delta + 3l\cos\delta\sin\delta \\ & - g^2 l\cos\delta\sin\delta + 8\eta^2\delta^2\frac{\cot\delta}{\sin\delta} + 4\eta^2\delta\cot\delta - 12\eta^2 l\cot\delta\Bigg) \end{aligned} \tag{1.14a}$$

$$\begin{aligned} \frac{d\delta}{dt} = {} & \frac{2g}{\pi\eta}\Bigg(2\eta^2\delta - 6l\eta^2 + 6l\eta^2\delta\cot\delta + 4\eta^2\frac{\delta^2}{\sin\delta} - l\delta\sin\delta + lg^2\delta\sin\delta \\ & - l\delta\cos\delta\sin\delta + 2l\sin^2\delta - g^2 l\sin^2\delta\Bigg), \end{aligned} \tag{1.14b}$$

$$\frac{\mathrm{d}g}{\mathrm{d}t} = \frac{2\eta}{\pi}\Bigg(-2 + g^2 + \frac{\delta^2}{\sin^2\delta} + 6\eta^2\frac{1}{\sin^2\delta} - 3\eta^2\frac{\delta^2}{\sin^4\delta} - \delta^2\cot^2\delta + 3\eta^2\delta^2\frac{\cot^2\delta}{\sin^2\delta} + 2\delta\cot\delta - g^2\delta\cot\delta - 6\eta^2\delta\frac{\cot\delta}{\sin^2\delta}\Bigg). \tag{1.14c}$$

$$\frac{\mathrm{d}a}{\mathrm{d}t} = -\frac{1}{2\sin\delta}\left(-\delta + 6\eta^2\delta + \delta\cos 2\delta + 4g^2\sin\delta - \sin 2\delta + g^2\sin 2\delta\right). \tag{1.14d}$$

In the above equations, the shelf length l is not fixed yet. In order to determine its value, we note that the differential Eqs. (1.14a)–(1.14d) exhibit a fixed point which corresponds to the exact stationary soliton solution of the NLCME

$$\eta = \frac{\sin\delta_{\mathrm{fp}}}{\sqrt{3}}, \tag{1.15a}$$

$$\delta = \delta_{\mathrm{fp}}, \tag{1.15b}$$

$$g = 0, \tag{1.15c}$$

$$a = t\cos\delta_{\mathrm{fp}}. \tag{1.15d}$$

Moreover, the value of δ_{fp} can be calculated with the help of the energy conservation law. According to Eq. (1.9), the energy of the pulse described through Eqs. (1.10a) and (1.10b) is

$$\mathcal{E} = 4\eta^2\frac{1}{\sin\delta}(2 - \delta\cot\delta) - 12\eta^4\frac{1}{\sin^3\delta}(1 - \delta\cot\delta) - 4\eta^2 g^2\frac{1}{\sin\delta} - 8\eta^2 g^2\frac{\delta}{\sin^2\delta} + 2g^2 l - 3g^4 l. \tag{1.16}$$

Upon equating the energy at the fixed point $\varepsilon_{\mathrm{fp}} = 4\sin\delta_{\mathrm{fp}}/3$ with the energy of the initial pulse, we obtain for δ_{fp}:

$$\delta_{\mathrm{fp}} = \arcsin\left(3\eta_0^2\frac{1}{\sin\delta_0}(2 - \delta_0\cot\delta_0) - 9\eta_0^4\frac{1}{\sin^3\delta_0}(1 - \delta_0\cot\delta_0)\right). \tag{1.17}$$

Now, in order to obtain the oscillation frequency ω of the variational parameters, we linearize Eq. (1.14) around δ_{fp}, leading to

$$\omega = \frac{2}{\sqrt{3}\pi}\sqrt{(3l - 4\delta_{\mathrm{fp}} - 3l\cos\delta_{\mathrm{fp}} - 2\sin\delta_{\mathrm{fp}})(2\delta_{\mathrm{fp}}\cos\delta_{\mathrm{fp}} + (\delta_{\mathrm{fp}}^2 - 2)\sin\delta_{\mathrm{fp}})}. \tag{1.18}$$

This allows us to finally deduce the length of the shelf by comparing this frequency with the actual oscillation frequency $\omega = 1 - \cos\delta_{\mathrm{fp}}$ of the soliton, which represents

the nonlinear frequency shift of the pulse [3]. Consequently, we obtain the length l of the shelf as

$$l = \frac{\pi^2}{4}\frac{1-\cos\delta_{fp}}{2\delta_{fp}\cos\delta_{fp}+(\delta_{fp}^2-2)\sin\delta_{fp}} + \frac{4\delta_{fp}+2\sin\delta_{fp}}{3(1-\cos\delta_{fp})}. \tag{1.19}$$

The above expression (1.19) for the shelf length diverges at $\delta_{fp} \approx 0.66\pi$ and it becomes even negative for larger values of the detuning. The reason of this singular behavior originates from the instabilities of the gap solitons in the lower half of the band gap. However, since we consider only the limit of small detunings, this unphysical behavior is of no relevance to our case.

1.3 Radiation Losses

To include the radiation loss in our calculation, we have to couple the nonlinear radiation modes to the linear modes of the system as discussed above. The linear modes represent the solutions of the linearized coupled mode equations (LCME)

$$i\frac{\partial E_+^r}{\partial z} + i\frac{\partial E_+^r}{\partial t} + E_-^r = 0, \tag{1.20a}$$

$$-i\frac{\partial E_-^r}{\partial z} + i\frac{\partial E_-^r}{\partial t} + E_+^r = 0. \tag{1.20b}$$

Here, $E_\pm^r$ denotes, respectively, the dispersive radiation in forward and backward propagating modes in the regions to the left and the right of the shelf. Then, the mass propagating to the right of the pulse is given by

$$\frac{\mathrm{d}}{\mathrm{d}t}\int_{l/2}^{\infty}(|E_+^r|^2+|E_-^r|^2)\mathrm{d}z = |E_+^r(z=l/2,t)|^2 - |E_-^r(z=l/2,t)|^2. \tag{1.21}$$

This equation describes the non-Markovian radiation dynamics of the solitary wave formation process alluded to above: Radiation travels away from the pulse further to the right (E_+^r), but may become back-reflected from the PBG material so that certain parts of it (E_-^r) return to the pulse. Eventually, only the difference of the masses contained in the modes associated with E_+^r and E_-^r can actually leave the pulse. Since the pulse is symmetric, the radiation propagating to the left exhibits the same behavior. Therefore, in order to allow the coupling of the nonlinear radiation modes to the linear radiation modes, we have to modify the mass conservation of our variational approach to allow for this effect according to

$$\frac{\mathrm{d}}{\mathrm{d}t}\left(4\eta^2\frac{\delta}{\sin^2\delta}+2g^2l\right) = -2\,|E_+^r(z=l/2,t)|^2 + 2\,|E_-^r(z=l/2,\,t)|^2. \tag{1.22}$$

On the r.h.s. of Eq. (1.22), only the radiation part occurs. The l.h.s. of Eq. (1.22) represents the mass conservation law within the variational approach which results

from inserting the trial functions into Eq. (1.8). Alternatively, the same expression can be derived directly from Eq. (1.14).

Due to the fact that near the upper band edge we can reduce the NLCME to the Nonlinear Schrödinger equation (NLSE), we may now write [3]

$$\begin{pmatrix} E_+^r(z,\,t) \\ E_-^r(z,\,t) \end{pmatrix} = \frac{1}{\sqrt{2}}\left(a^r(z,\,t)\begin{pmatrix} 1 \\ -1 \end{pmatrix} - \frac{i}{2}\frac{\partial a^r(z,\,t)}{\partial z}\begin{pmatrix} 1 \\ 1 \end{pmatrix}\right) \mathrm{e}^{-it}, \tag{1.23}$$

where a^r denotes the solution of the linearized NLSE. Upon inserting Eq. (1.23) into the r.h.s. of Eq. (1.21) we obtain

$$2\,|E_+^r(z=l/2,\,t)|^2 - 2\,|E_-^r(z=l/2,\,t)|^2 = -2\,\mathrm{Im}\,(a^{r*}\,a_z^r)|_{z=l/2}. \tag{1.24}$$

The corresponding calculation for the r.h.s. of Eq. (1.22) is identical to that presented in Ref. [12], where radiation losses for the NLSE – as opposed to the present analysis of the NLCME – have been investigated. As a result, the modified mass conservation equation of the NLCME takes the form (see Ref. [12])

$$\frac{\mathrm{d}}{\mathrm{d}t}\left(4\eta^2\frac{\delta}{\sin^2\delta} + 2g^2 l\right) = -2r\frac{\mathrm{d}}{\mathrm{d}t}\int_0^t \frac{r}{\sqrt{\pi(t-t)}}\,\mathrm{d}t, \tag{1.25}$$

where the height r of the shelf is defined as

$$r^2 = |a^r(z=l/2,\,t)|^2 = |E_+^r(z=l/2,\,t)|^2 + |E_-^r(z=l/2,\,t)|^2. \tag{1.26}$$

Following the argumentation of Ref. [12], the radiation losses may be introduced to the differential equation for the shelf g by adding to its r.h.s. the loss term $-2\beta g$

$$\begin{aligned}\frac{\mathrm{d}g}{\mathrm{d}t} = \frac{2\eta}{\pi}\Bigg(&-2 + g^2 + \frac{\delta^2}{\sin^2\delta} + 6\eta^2\frac{1}{\sin^2\delta} - 3\eta^2\frac{\delta^2}{\sin^4\delta} - \delta^2\cot^2\delta \\ &+ 3\eta^2\delta^2\frac{\cot^2\delta}{\sin^2\delta} + 2\delta\cot\delta - g^2\delta\cot\delta - 6\eta^2\delta\frac{\delta}{\sin^2\delta}\Bigg) - 2\beta g.\end{aligned} \tag{1.27}$$

What remains is to derive an expression for the height r of the shelf and the loss coefficient β within our variational approach to the NLCME. The mass conservation can be rewritten as (recall that in our case $\delta \ll 1$)

$$\frac{\mathrm{d}}{\mathrm{d}t}\left(4\eta^2\frac{\delta}{\sin^2\delta} + 2\lg^2\right) \approx \frac{\mathrm{d}}{\mathrm{d}t}\left(4\frac{\eta^2}{\delta} + 2\lg^2\right). \tag{1.28}$$

Then, for small derivations of the parameters from the fixed point η_1 and δ_1, we obtain

$$\frac{\mathrm{d}}{\mathrm{d}t}\left(4\frac{\eta^2}{\delta} + 2\lg^2\right) \approx \frac{8}{3\delta_{\mathrm{fp}}}\left(1 + \frac{32}{3\pi^2}\right)\frac{\mathrm{d}}{\mathrm{d}t}\left(2\eta_1^2 + 2\frac{9\pi^2}{64}g^2\right). \tag{1.29}$$

Moreover, the linearized Eq. (1.21) for g and η_1 give

$$\eta_1 = -\frac{r}{\sqrt{2}}\sin\phi, \tag{1.30a}$$

$$g = -\frac{8}{3\pi}\frac{r}{\sqrt{2}}\cos\phi, \tag{1.30b}$$

where the angle ϕ determines the (temporal) oscillatory behavior of the functions g and $\eta 1$. Finally, by combining Eqs. (1.25),(1.29) and (1.30) we obtain the decay factor β as

$$\beta = \left(\frac{3\pi}{8}\right)^2 \frac{r}{2r(0)\, l\sqrt{\pi t}}, \tag{1.31}$$

with

$$r^2 = \frac{3\,\delta_{\mathrm{fp}}}{8}\frac{1}{1+\dfrac{32}{3\pi^2}}\left(\frac{4}{3}\,\delta_{\mathrm{fp}} - 2\lg^2 - 4\eta^2\frac{\delta}{\sin^2\delta}\right). \tag{1.32}$$

This completes the calculation of the radiation losses and we have obtained a closed set of equations of motion, Eqs. (1.14a), (1.14b), (1.14d) and (1.27), together with Eqs. (1.17), (1.19), (1.31), and (1.32) as well as the initial conditions, Eq. (1.11a) and (1.11b).

1.4 Results

In order to compare the results of our variational approach with numerically exact results, we analyze the maximum intensity $I_{\max}(t)$ of the pulse starting with the same initial conditions. Owing to the symmetry of the problem, this maximum always occurs at the origin and within the variational approach it is given as

$$I_{\max}(t) = I(z=0,\, t) = 2\left|\frac{\eta}{\cos(\delta/2)} + ig\right|^2. \tag{1.33}$$

In Figure 1.1 we compare the evolution of a pulse (initial conditions $\delta_0 = 0.1\pi$ and $\eta_0 = 1.01\,\sin(0.1\pi)/\sqrt{3}$) within a numerically exact solution of the NLCME [13] (dashed blue line) and our variational approach (solid red line).

For relatively short times, the variational equations describe the wave dynamics rather accurately. However, for longer times the results become successively less accurate. This is a consequence of the approximations that have reduced the radiation losses of the NLCME model to those of the NLSE, i.e., Eq. (1.27). In other words, for long time scales, the NLSE model becomes an inaccurate approximation to the NLCME model, since the NLSE model does not properly account for the dispersion relation of the linear modes near the PBG. As a result, the expected non-Markovian effects are lost in this case. This is in contrast to the situation without losses, where the NLCME maps exactly to the NLSE for frequencies near the PBG.

In order to restore the correct quantitative behavior for long times, a more sophisticated treatment of losses has to be developed. Specifically, the LCME have to be solved without using the NLSE reduction.

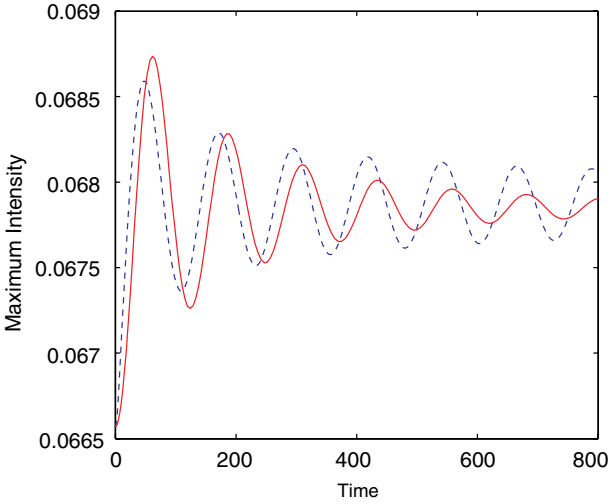

Figure 1.1 Comparison of the losses of the variational solution (solid line) with the direct numerical solution of the NLCME (dashed line). The maximum intensity $I_{max}(t)$ is plotted as a function of the dimensionless time for an initial pulse with $\delta_0 = 0.1\pi$ and $\eta_0 = 1.01\, sin\,(0.1\pi)/\sqrt{3}$.

1.5 Conclusions and Outlook

To summarize, we have presented the variational approach to relaxation of arbitrary pulses to exact solitary wave solutions in one-dimensional PBG materials within the NLCME model. For frequencies near the band edge, we have treated losses to linear radiation modes within the NLSE model. This approach allows a quantitatively correct description of the wave dynamics for not too long time scales. However, for long time scales, the results become less and less accurate, although still remaining qualitatively correct. This is somewhat surprising since naively one would expect that near band edges the NLCME results reduce to the NLSE results. In fact, this is the case for problems without radiation losses such as in the nonresonant collision of Bragg and/or gap solitons [14,15]. However, if the coupling to linear radiation modes is important, for long time scales the oversimplified dispersion relation inherent in the NLSE model fails to correctly take into account the non-Markovian radiation dynamics associated with strong Bragg scattering in nonlinear and/or coupled systems. Therefore, future progress has to be based on a more accurate treatment of these memory effects.

Acknowledgements

We acknowledge support by the Center for Functional Nanostructures (CFN) of the Deutsche Forschungsgemeinschaft within project A1.2. The research of L.T. and K.B.

is further supported by the DFG-Priority Program SPP 1113 "Photonic Crystals" under grant No. Bu-1107/6-1.

References

1 Joannopoulos, D. Meade, R.D. and Winn, J.N. (1995) *Photonic Crystals: Molding the Flow of Light*, Princeton University Press, Princeton, NJ.

2 Busch, K. *et al*. (2007) *Phys. Rep*. **444**, 101.

3 de Sterke C.M. and Sipe, J.E. (1994) in *Progress in Optics*, Vol. 33 (ed. E. Wolf), Elsevier Science, Amsterdam p. 203.

4 Chen W. and Mills, D.L. (1987) *Phys. Rev. Lett*. **58**, 160.

5 Eggleton, B.J. *et al*. (1996) *Phys. Rev. Lett*., **76**, 1627.

6 Mok, J.T. *et al*. (2006) *Nature Physics*, **2**, 775.

7 Barashenkov, I.V. Pelinovsky, D.E. and Zemlyanaya, E.V. (1998). *Phys. Rev. Lett*. **80**, 5117.

8 Quang T. and John, S. (1994). *Phys. Rev. A* **50**, 1764.

9 Vats, N. John, S. and Busch, K. (2002). *Phys. Rev. A*, **65**, 043808.

10 Gelfand I.M. and Fomin, S.V. (1963). *Calculus of Variations*, Prentice-Hall, Englewood Cliffs, NJ.

11 Malomed, B.A. (2002)in *Progress in Optics* Vol. 43 (ed. E. Wolf,), Elsevier Science, Amsterdam, p. 71.

12 Kath W.L. and Smyth, N.F. (1995) *Phys. Rev. E*, **51**, 1484.

13 de Sterke, C.M. Jackson, K.R. and Robert, B.D. (1991) *J. Opt. Soc. Am. B*, **8**, 403.

14 Tkeshelashvili, L. Pereira, S. and Busch, K. (2004) *Europhys. Lett*., **68**, 205.

15 Tkeshelashvili, L. *et al*. (2006) *Photon. Nanostruct.: Fundam. Appl*., **4**, 75.